Theor. Appl. Climatol. 74, 93–103 (2003)
DOI 10.1007/s00704-002-0714-4

Theoretical and Applied Climatology

Printed in Austria

[1] Department of Atmospheric Sciences, University of Buenos Aires, Ciudad Universitaria, Buenos Aires, Argentina
[2] Department of Atmospheric Sciences/Centro de Investigaciones del Mar y la Atmósfera (CIMA), University of Buenos Aires – CONICET, Ciudad Universitaria, Buenos Aires, Argentina

Objective method for classifying air masses: an application to the analysis of Buenos Aires' (Argentina) urban heat island intensity

R. A. Bejarán[1] and **I. A. Camilloni**[2]

With 3 Figures

Received October 24, 2001; revised June 12, 2002; accepted October 10, 2002
Published online January 17, 2003

Summary

During recent years, numerous studies have examined the Buenos Aires urban climate, but the relationship between large-scale weather conditions and the Buenos Aires urban heat island (UHI) intensity has not been studied. The goal of this paper is to apply an objective synoptic climatological method to identify homogeneous air masses or weather types affecting Buenos Aires during winter, and to relate the results to the UHI intensity. A K-means clustering method was used to define six different air masses considering the 03:00, 09:00, 15:00 and 21:00 LT surface observations of dry bulb temperature, dew point, cloud cover, atmospheric pressure and wind direction and velocity at Ezeiza, the most rural meteorological station of the Buenos Aires metropolitan area (Fig. 1). Results show that the mean UHI intensity is at its maximum (2.8 °C) a few hours before sunrise when conditions are dominated by cold air masses associated with cold-core anticyclones, weak winds and low cloud cover. Inverse heat islands are found during the afternoon for all air masses indicating that surface processes are not dominant at that time. The relatively infrequent and warmest air mass is the only one that presents a mean negative urban-rural temperature difference (− 0.1 °C) during the afternoon with the smallest diurnal cycle of the UHI intensity probably due to the prevailing high humidity and cloudy sky conditions. The paper provides an insight into the Buenos Aires urban–rural temperature difference under a variety of winter weather types and results could be useful to improve local daily temperature forecasts for the metropolitan area of Buenos Aires on the basis of the routine forecasts of weather types.

1. Introduction

Urbanization processes produce many changes in the surface nature and in the properties of the local atmosphere. These processes involve an alteration of the local climate as a result of the transformations in radiative, thermal, moisture and aerodynamic characteristics of the surface and changes in the turbulent fluxes of momentum, heat and water vapor. Nevertheless the urban climate at any locality is generally governed by the large-scale weather conditions. The interaction between the synoptic scale and the local scale is a continuous seesaw: sometimes the large-scale weather conditions are dominant and at others the local conditions are prevalent (Landsberg, 1981). For example, Lowry (1977) pointed out the fact that the weather type situation should be considered in conducting statistical studies of the urban effect on temperature.

One of the most noticeable consequences of urban growth is the consistent rise in the urban

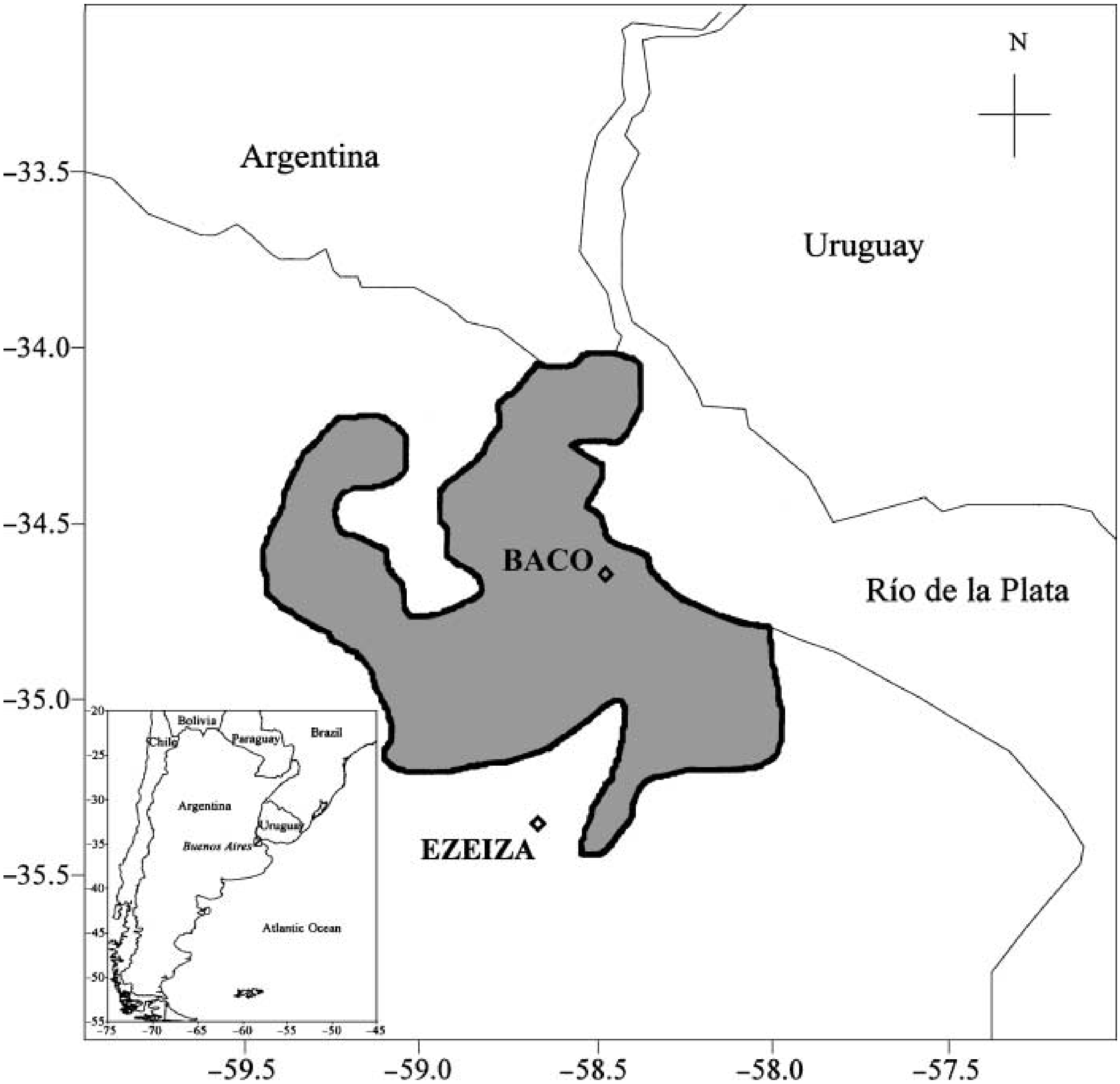

Fig. 1. Map of Buenos Aires metropolitan area (▩) and location of meteorological stations considered in this study: Buenos Aires Central Observatory (BACO) and Ezeiza

temperature (i.e. Bornstein, 1968; Oke, 1979; Colacino and Rovelli, 1983; Karl et al., 1988; Barros and Camilloni, 1994; Camilloni and Barros, 1997; Figuerola and Mazzeo, 1998). The different surface structure between the urban and surrounding rural environment produces the well-known urban heat island (UHI) phenomenon. Oke (1982) lists a number of factors contributing to the UHI, including altered energy balance terms leading to positive thermal anomaly, anthropogenic heat sources, increased sensible heat storage, decreased evapotranspiration due to construction materials and decreased total turbulent heat transport due to wind speed reduction caused by canyon geometry. In addition, the dependency of the UHI effect on wind speed, cloud cover and the near-surface lapse rate has been studied by many authors (i.e. Sundborg, 1950; Chandler, 1965; Oke, 1973; Lee, 1975; Godowitch et al., 1985; Moreno-García, 1994; Kidder and Essenwanger, 1995; Camilloni, 1999; Runnalls and Oke, 2000; Morris et al., 2001). These studies show that wind speed and the amount of cloud cover are the most significant meteorological parameters controlling the intensity and development of the UHI. This is because these variables define the ventilation and insolation in and around the urban region. Oke (1998) showed that by holding the effects of clouds constant, by only using cloudless data, there is an inverse relationship between the UHI intensity and wind speed that generally fits an inverse square root form. Runnalls and Oke (2000) studied Vancouver's UHI and showed that to represent the effect of cloud it is important to consider cloud amount and type because they both affect the surface radiative cooling by decreasing longwave radiative losses. Combining the wind speed and cloud effects, Oke (1998) developed a weather factor that expresses the degree to which weather controls reduce the UHI intensity. Morris et al. (2001) quantified the influences of wind and cloud on Melbourne's UHI and showed that the UHI was inversely proportional to about the fourth root of the wind speed and the amount of cloud. Although the distinct physical and anthropogenic characteristics of each urban environment probably mean these results are not necessarily applicable for all urban areas, they all show that the combination of clear sky and calm wind results in the largest UHI values. Increased cloud limits the UHI development by limiting the nocturnal radiative cooling while increases in the wind speed result in larger urban mixing and in a restriction of the development of the UHI.

Buenos Aires (Argentina) is one of the world's largest cities. The metropolitan area extends for around 4000 km^2 and has 12.5 million inhabitants. Its surface is featureless with only minor differences in height of less than 30 m and is located around 35° S along the western coast of the Río de la Plata estuary (Fig. 1). Recently some studies have been conducted on the urban climate of Buenos Aires but the relationship between the large-scale weather conditions and its UHI intensity has not been studied yet. A better knowledge of the UHI intensity under different weather conditions may be an important tool for routine local temperature forecasts, which generally include the urban effect on temperature, assuming a standard difference of 2 °C between the urban and rural minimum temperatures. The goal of this paper is to apply an objective synoptic climatological method to identify homogeneous air masses or weather types affecting Buenos Aires during winter and to relate the results to the UHI intensity. Information from this study on the linkages between the different weather types that affect Buenos Aires during winter and the UHI intensity could contribute to more accurate temperature forecasts for the Buenos Aires metropolitan area and also be of economic interest to evaluate daily urban energy demands.

2. Data and methodology

Six-hourly meteorological data for the austral winter months June–July–August for the period 1959–91 were collected from two stations located in Buenos Aires: Buenos Aires Central Observatory (BACO) and Ezeiza (see Fig. 1). Both stations perform routine meteorological observations and are operated by the National Weather Service. Table 1 presents the geographic coordinates of each station with a description of its urban/rural character. The austral wintertime was selected because it has the greatest variety of synoptic situations that might affect Buenos Aires. Moreover, the results of Figuerola and Mazzeo (1998) show that the daily urban–rural temperature difference in Buenos Aires reaches its maximum value during winter.

There are some relevant research papers in the scientific literature that explicitly examined the

Table 1. Location and environmental description of the meteorological stations considered in this study

Meteorological station	Geographic coordinates	Environmental description
Buenos Aires Central Observatory	34°35′S, 58°26′W	Located in the geographical city center, in a park of 0.4 km^2 and in a corner of one of the largest parks in the city of around 4 km^2. The nearest surrounding buildings have no more than four floors and the nearest building is situated at 20 m. Meteorological observations are made over low grass.
Ezeiza	34°49′S, 58°32′W	Located in the area of the international airport of Buenos Aires where the surrounding environment is rural. The nearest building is 600 m to the southeast. Meteorological observations are made over low grass.

interaction between the prevailing synoptic conditions and the UHI magnitude (for example, Unwin, 1980; Yague et al., 1991; Unger, 1996 and Morris and Simmonds, 2000). Unwin (1980) investigated the variations in the UHI of Birmingham UHI for Lamb's eleven weather types (Lamb, 1972) determined by the airflow characteristics. Yague (1991) considered three synoptic types to analyze two years of data of Madrid's UHI. Unger (1996) distinguished thirteen weather types to analyze the UHI intensity of the medium-sized town of Szeged in Hungary. These studies show that for the three different cities the highest UHI values were associated with anticyclonic conditions and that cyclonic conditions associated with windy weather resulted in lower UHI values. Morris and Simmonds (2000) grouped Melbourne's UHI intensity into six categories and analyzed the prevailing synoptic conditions for each category. They showed that the groups with the stronger UHI were associated with synoptic conditions with low cloud cover and weak winds but, unlike the previously mentioned studies, the weakest UHI events were not associated with cyclonic conditions.

Synoptic climatology studies the relationships between the atmospheric circulation and the surface environment and therefore it has a great potential to help to explain the key interaction between the regional atmospheric circulation and the local weather. There is no unique or optimal way for classifying air masses or weather types. Yarnal (1993, 2001) reviews a large number of synoptic classification techniques: manual typing, correlation-based analyses, eigenvector-based analyses (principal components analysis, empirical orthogonal functions, discriminant analysis and cluster analysis), compositing, indexing, spatial synoptic climatology and synoptic dendroclimatology. Some authors have applied different synoptic classification techniques for classifying air masses with different purposes. For example, Greene et al. (1999) used an automated synoptic classification to analyze the impact of different weather types on atmospheric pollution at four US cities and Kalkstein et al. (1996, 1998) developed the Spatial Synoptic Classification for classifying days at a particular location into distinct air masses categories and integrating these classifications over a larger domain into spatially cohesive air mass regions. Sheridan et al. (1999) used Kalkstein et al.'s (1996) scheme to evaluate the spatial and temporal variability of air masses between urban and rural areas in northeastern US. Kalkstein et al. (1987) evaluated three clustering techniques (Ward's, average linkage and centroid) for the determination of homogeneous synoptic classes. Dorling et al. (1992a, 1992b) applied cluster analysis to estimate the synoptic controls on air and precipitation chemistry for Southern Scotland and Brook et al. (1995a, 1995b) used cluster analysis of three-day progressions of 850 hPa wind flow over eastern North America to examine wet deposition of pollutants.

In this paper, we use the K-means clustering method (Mc Queen, 1967; Michelangeli et al., 1995; Robertson and Ghil, 1999). An advantage of this partitioning method is that it classifies *all* days into a predefined number of clusters in a way that minimizes the sum of squared distances within the members of each cluster and maximizes this quantity among the members of different clusters. This method of clustering is very different from the joining methods (i.e. single linkage, complete linkage, Ward's) as the kind of research questions that can be addressed must include an hypothesis concerning the number of clusters that will be produced. A complete description of the algorithms for the K-means procedure can be found in Spath (1980).

The K-means method was applied to the 03:00, 09:00, 15:00 and 21:00 LT (local time) surface observations of dry bulb temperature, dew point, cloud cover, atmospheric pressure and wind direction and velocity at Ezeiza, the most rural meteorological station of the Buenos Aires metropolitan area (Fig. 1). Because the different variables included here used different types of scales, the data were standardized so that each variable has a mean of 0 and a standard deviation of 1. It is very important that the variables used to compute the distances between objects are of comparable magnitude; otherwise the analysis will be biased and rely more heavily on the variables that have the greatest range of values. In this study we hypothesize that the number of different synoptic patterns that could affect the Buenos Aires metropolitan area is six, and then we predefined that the number of clusters (K) is six. As the K-means method classifies all days, there is no category for transitional or unclassified days.

3. Winter air masses classification

Six air mass types were defined and the mean and standard deviations values for the 24 meteorological variables within each cluster were calculated (Table 2). It can be seen that standard deviation values are proportional to their corresponding means. In order to have a better understanding of the circulation fields associated with each air mass, the sea level pressure (SLP) field for one hour and day of each air mass type, chosen arbitrarily among those with the shortest distances within each cluster, are presented in Fig. 2. SLP data are from the NCEP (National Centers for Environmental Prediction) reanalyses (Kalnay et al., 1996) that are available on a $2.5° \times 2.5°$ latitude–longitude grid.

The winter air masses that affect Buenos Aires are:

i) **C++** (very cold), defined by cluster 1 appears to be a polar air mass with the lowest temperatures, low cloud cover or clear skies, light winds and very dry conditions. This air mass is generally advected from the S–SW through circulation around a cold-core anticyclone. An important and distinct geographical feature of the South American continent is the presence of the Andes, a steep and narrow mountain range extending all the way along the west coast. The air masses C++ that affect Buenos Aires originate in the intense Pacific Ocean surface anticyclones that cross the Andes and Argentina south of 35° S and take a northeastern direction during the winter months. This air mass is initially a polar maritime air mass that is modified during its continental trajectory,

Table 2. Mean values of the meteorological variables (T: temperature, T_d: dew point, p: sea-level pressure, cc: cloud cover, u: E–W wind component, v: N–S wind component) for the six clusters. ($u>0$ represents westerly winds and $v>0$ represents southerly winds)

	Cluster 1 (C++)		Cluster 2 (S)		Cluster 3 (W+)		Cluster 4 (SW)		Cluster 5 (W++)		Cluster 6 (SE)	
	mean	st. dev.	mean	st. dev.	mean	st. dev.	mean	st. dev.	mean	st. dev.	mean	st. dev.
T_{03} (°C)	2.1	1.5	11.9	1.7	7.0	1.7	7.3	1.8	13.8	1.8	7.1	1.7
T_{09} (°C)	1.8	1.6	11.5	1.5	7.5	1.7	6.2	1.7	14.3	1.7	7.3	1.6
T_{15} (°C)	12.2	1.6	14.4	1.6	17.2	1.6	13.2	1.8	19.9	1.9	12.4	1.6
T_{21} (°C)	5.6	1.5	10.9	1.4	10.8	1.5	7.1	1.6	16.2	1.6	8.7	1.5
$T_{d\,03}$ (°C)	0.1	1.6	10.4	1.8	4.5	1.6	4.7	1.9	11.5	1.8	5.7	1.7
$T_{d\,09}$ (°C)	– 0.2	1.6	10.3	1.6	4.8	1.7	3.4	1.8	12.2	1.7	5.8	1.6
$T_{d\,15}$ (°C)	1.3	1.8	10.6	1.6	6.5	1.8	2.7	1.9	14.0	1.6	6.8	1.7
$T_{d\,21}$ (°C)	1.9	1.6	9.1	1.6	7.0	1.6	2.6	1.7	13.8	1.5	6.6	1.7
p_{03} (hPa)	1025.9	2.1	1011.6	2.2	1019.1	2.0	1013.0	2.2	1014.7	2.2	1021.6	2.1
p_{09} (hPa)	1026.9	2.1	1011.9	2.1	1019.2	2.0	1015.1	2.1	1014.1	2.3	1022.4	2.0
p_{15} (hPa)	1025.3	2.0	1010.7	2.2	1016.7	2.1	1014.9	2.1	1011.2	2.3	1021.0	2.0
p_{21} (hPa)	1025.6	2.1	1012.8	2.2	1016.8	2.1	1017.3	2.2	1011.6	2.3	1021.8	2.1
u_{03} (kt)	1.3	1.8	– 1.8	2.1	0.8	1.8	6.1	2.3	– 3.2	2.1	– 2.3	1.9
u_{09} (kt)	1.4	1.7	– 1.4	2.2	0.7	1.8	6.8	2.3	– 2.7	2.1	– 2.9	2.1
u_{15} (kt)	1.5	2.4	– 0.5	2.5	1.8	2.4	10.4	2.5	– 1.6	2.4	– 5.2	2.3
u_{21} (kt)	– 0.3	1.8	0.4	2.3	– 0.7	1.9	4.7	2.1	– 2.8	2.1	– 3.7	2.2
v_{03} (kt)	0.9	1.9	0.3	2.5	– 3.1	2.0	1.0	2.5	– 5.4	2.3	3.2	2.3
v_{09} (kt)	0.5	1.9	2.3	2.4	– 3.7	2.0	2.0	2.2	– 5.7	2.2	3.1	2.3
v_{15} (kt)	0.4	2.6	4.4	2.6	– 5.6	2.3	6.0	2.5	– 6.3	2.3	3.2	2.6
v_{21} (kt)	– 0.6	1.8	4.2	2.5	– 3.3	2.0	0.9	2.3	– 2.6	2.4	2.6	2.2
cc_{03} (oktas)	1.5	1.5	7.0	1.4	1.7	1.5	4.0	1.8	5.2	1.7	5.6	1.7
cc_{09} (oktas)	2.3	1.6	7.6	1.1	3.5	1.7	4.4	1.7	6.6	1.4	7.0	1.3
cc_{15} (oktas)	3.2	1.6	7.2	1.3	3.8	1.7	3.7	1.7	6.7	1.4	6.9	1.3
cc_{21} (oktas)	1.9	1.6	5.9	1.7	2.9	1.7	2.2	1.6	6.1	1.5	5.8	1.7

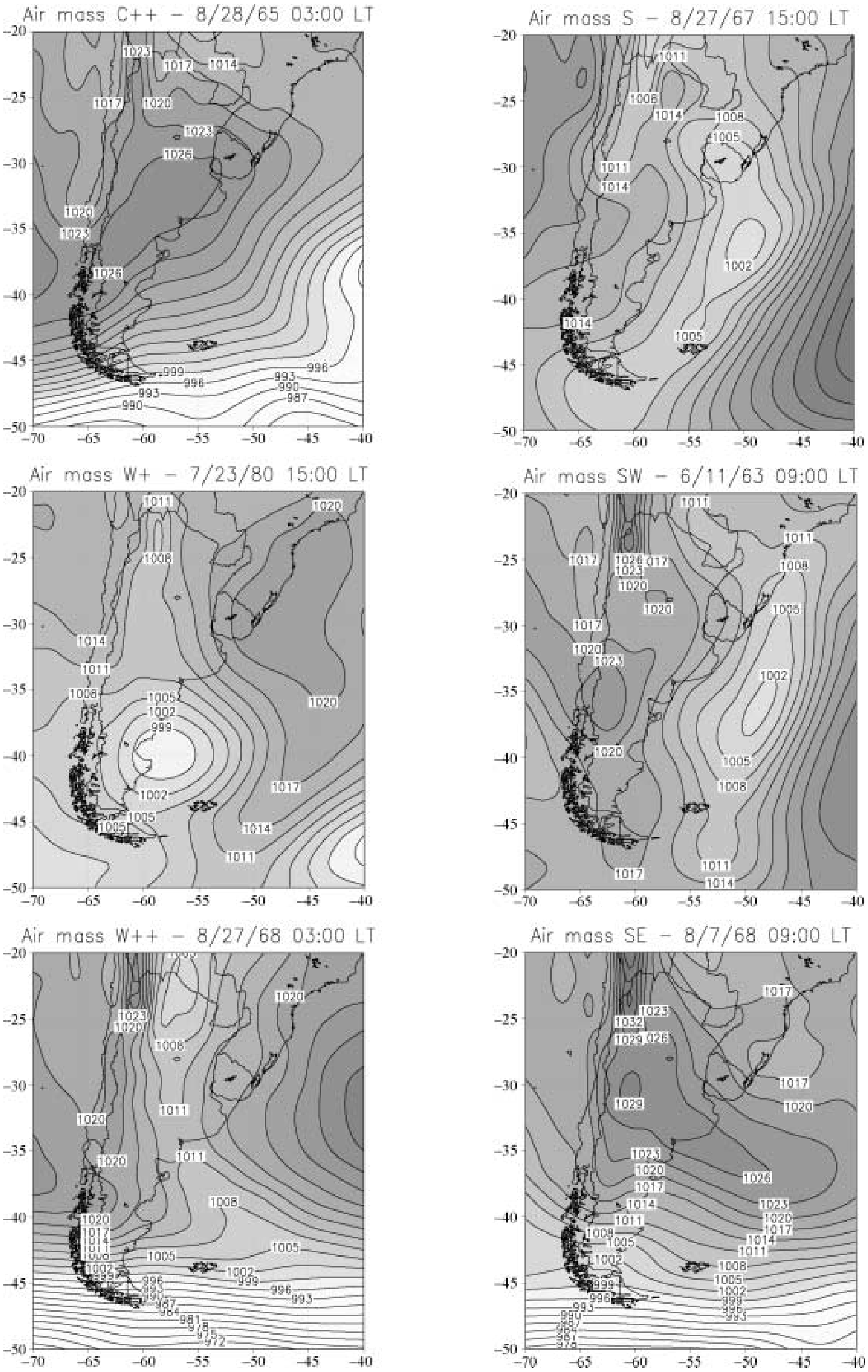

Fig. 2. Mean sea-level pressure fields for selected days of the six different air masses classified

becoming drier and arriving at Buenos Aires as a dry polar continental air mass.

ii) Cluster 2 defines a second type of air mass named **S** (southern) associated with prevailing southern wind and a low pressure system located to the east of Buenos Aires. In spite of the southern wind, temperatures are relatively warm due to the air mass trajectory over the Atlantic Ocean and the high cloud that inhibits the nocturnal cooling. The diurnal temperature amplitude is small (3.5 °C) and weather conditions are humid due to water vapor advection from the S–SE.

iii) **W+** (warm) defined by cluster 3 is a relatively warm air mass during the afternoon hours due to the warm advection from the

N–NW as a consequence of a trough in the center of Argentina and the intense subtropical anticyclone in the east. This air mass exhibits a large mean daily temperature amplitude (10.2 °C), above normal surface pressure and low cloud cover amounts.

iv) The air mass type defined by cluster 4, named **SW** (southwestern) is typical of overrunning cold frontal systems with increasing pressure and declining total cloud cover and moisture, low temperature and persistent SW winds. The intense southwestern wind associated to this synoptic situation is known as 'pampero' wind.

v) **W++** (very warm) is the warmest winter air mass defined by cluster 5. It has the highest mean temperature and dew points of all clusters. The typical weather conditions are high humidity and cloud cover, declining surface pressure and winds prevailing from the NE sector, typical of a tropical maritime air mass originating over the tropical South Atlantic Ocean and advected to Argentina through Brazil. This air mass is associated to the warm sector of a frontal system.

vi) Cluster 6 defines a **SE** (southeastern) air mass type that resembles cluster 2 with southeastern surface winds and skies virtually overcast. However, several differences exist. First, sea level pressure is above normal associated to a migratory anticyclone over central Argentina and the close Atlantic Ocean. Second, air temperatures are lower, especially at 03:00 LT and 09:00 LT, and the mean daily temperature amplitude is higher (5.3 °C) than in cluster 2. Third, the cloud type usually associated to SE air masses is low-level and stratus type.

Table 3 presents the frequency of occurrence of each air mass type as defined by the clustering method. W+, SE and C++ are the most common winter air masses that affect Buenos Aires. The occur on more than half of winter days (58.3%). The relatively warm S and W++ air masses are not unusual (29.7%). The SW air mass is the least frequent and, in statistical terms, it can be expected to affect Buenos Aires on no more than 13 days during winter.

Table 3. Air mass type frequencies (%)

Air mass type	Frequency (%)
C++	18.5
S	15.5
W+	21.1
SW	12.0
W++	14.2
SE	18.7

Table 4. Frequencies of permanence (%) for two consecutive days of each air mass type and frequencies of change (%) between all air masses identified. Largest values are bold

		Day +1					
		C++	S	W+	SW	W++	SE
Day 0	C++	**52.2**	0.9	25.6	2.8	0.7	17.7
	S	5.5	26.3	10.5	**26.7**	8.3	22.8
	W+	4.0	14.9	**44.7**	7.7	16.7	12.0
	SW	**33.5**	3.1	22.4	29.8	3.1	7.9
	W++	0.0	35.6	2.8	8.8	**47.7**	5.0
	SE	16.5	13.7	12.1	4.7	11.4	**41.6**

Table 4 presents the frequencies of permanence for two consecutive days of each air mass type and the frequencies of change between all the different air masses identified. Inspection of this table allows one to identify the air masses with higher persistency and the transitional ones. It can be seen that the most persistent air masses are C++ (52.2%), W+ (44.7%), W++ (47.7%) and SE (41.6%). The air masses S and SW mostly remain for only one day and therefore they can be considered as transitional. Table 4 also allows identification of the typical sequence of the air masses that affect Buenos Aires. Starting arbitrarily from the most frequent air mass W+, it can be expected an intensification of the northern flow with increasing temperatures and moisture associated to air masses W++. There is also a deepening of the trough over the continent and increasing cloud cover. W++ is the typical air mass of the warm sector of a frontal system that is replaced by an S air mass when the depression moves to the Atlantic Ocean. In the following stage, the S air mass is replaced by SW or SE air masses according to the trajectory of the post-frontal anticyclone that has two possible tracks in the region: SW–NE associated to extreme low temperatures in north-central Argentina and south Brazil or W–E with SE winds over Buenos Aires. Finally, these air

Table 5. Hourly frequencies (%) of $T_{BACO} > \overline{T}_{BACO}$ for each air mass type (T_{BACO} is the BACO temperature and $\overline{T}_{BACO}$ is the BACO average temperature over 1959–91)

	C++	S	W+	SW	W++	SE
03:00 LT	2.2	93.4	52.0	32.0	98.3	43.2
09:00 LT	1.8	94.2	57.4	23.7	99.5	43.4
15:00 LT	10.1	72.0	78.6	37.4	91.6	14.0
21:00 LT	7.0	64.3	72.9	14.6	85.4	33.0

masses are frequently replaced by C++ air masses with minimum cloud, temperature and moisture values, light winds and high surface pressure.

In order to evaluate the clustering method with independent data, the hourly frequency of $T_{BACO} > \overline{T}_{BACO}$ for each air mass type is presented in Table 5. $\overline{T}_{BACO}$ is the hourly average temperature for the 1959–91 period. Confirming the good performance of the clustering method, the major frequencies are observed for the warmer air masses S, W+ (mostly during the afternoon) and W++ while the smaller frequencies are associated to the colder ones (C++, SW and SE).

4. Buenos Aires' urban heat island intensity

The wintertime urban heat island effect in Buenos Aires is studied using the 03:00, 09:00, 15:00 and 21:00 LT surface observations from the Buenos Aires Central Observatory (urban) and Ezeiza (rural) meteorological stations. The urban site is within a park near the geographical centre of the actual urban area and the rural station is located at the international airport, 30 km southwest of the downtown area (see Fig. 1 and Table 1).

Table 6 presents the hourly mean Buenos Aires' UHI intensity (ΔT_{u-r}) and the corresponding standard deviation calculated with all days within each cluster. Most of the mean UHI intensities of the different air mass types are statistically different between them at the 95% level using a two-sided Student's t-test. The only exceptions are the C++ and S values at 15:00 LT, the W+ and SW values at 21:00 LT and the W+ and SE values at 03:00, 15:00 and 21:00 LT. In all cases, the UHI intensities are statistically different from zero at the 95% confidence level according to a two-tailed Student's t-test. In the mean, most of the classified air masses are associated with higher urban than rural temperatures. As expected for a good development of an urban heat island, the largest mean urban-rural temperature differences occur in anticyclonic conditions, light winds and low cloud cover prevailing during the night and early morning of C++ days. The UHI events are also strong when Buenos Aires is under the influence of the air masses W+ and SE that are also associated with relatively small wind speeds (<3 m/s) and anticyclonic conditions. Mean cloud cover values are quite different for these two air masses indicating in this case that wind speed is more relevant in determining the urban–rural temperature difference. The relatively cold air mass SW also shows well-developed UHI during the morning and night with a maximum mean value at 21:00 LT, when wind speed and cloud cover are at their minimum (2.4 m/s and 2.2 oktas respectively). The UHI is weakest during the NE flow regime of air masses W++ and often shows an inverse heat island or "cold island" during the afternoon when winds flow from the city towards the rural station. This effect was also found during the daytime by other authors (Camilloni and Mazzeo, 1987; Figuerola

Table 6. Hourly mean and standard deviation of the Buenos Aires' UHI intensity (ΔT_{u-r}) for each air mass type

	C++		S		W+		SW		W++		SE	
	mean	st. dev.	mean	st. dev.	mean	st. dev.	mean	st. dev.	mean	st. dev.	mean	st. dev.
$\Delta T_{u-r,03}$ (°C)	2.8	*1.3*	1.3	*1.1*	2.2	*1.3*	1.5	*1.1*	1.0	*1.2*	2.2	*1.2*
$\Delta T_{u-r,09}$ (°C)	2.7	*1.3*	1.1	*1.0*	1.8	*1.3*	1.4	*1.0*	0.5	*0.8*	1.8	*1.0*
$\Delta T_{u-r,15}$ (°C)	0.4	*0.9*	0.4	*0.7*	0.1	*1.0*	0.8	*0.5*	*−0.1*	*0.8*	0.2	*0.8*
$\Delta T_{u-r,21}$ (°C)	2.3	*1.2*	1.4	*1.0*	2.1	*1.3*	2.0	*1.1*	1.2	*1.0*	1.7	*1.1*

and Mazzeo, 1998) who analysed 24-h data. Figuerola and Mazzeo (1998) showed that there is a peak frequency of negative urban–rural temperature differences at 15:00 LT during wintertime. This is the time of occurrence of maximum daily temperature during winter days and negative or very low values of $\Delta T_{u-r,15}$ indicate that surface processes are not dominant during this time and consequently urban effects are almost absent. The air mass W++ presents the maximum UHI intensity at 21:00 LT when the hourly wind speed reaches its minimum value (1.9 m/s). With the southerly moist regime of S air masses, the UHI effect is relatively weak and reaches its maximum value during the first hours after sunset, probably due to the increased nocturnal radiative loss caused by the reduction in the amount of cloud (see Table 2).

Table 7 presents the hourly frequency (%) of $\Delta T_{u-r} > 0$ for each air mass type. Results confirm that the UHI is a nocturnal and early-morning phenomenon in Buenos Aires. In general it finds its largest intensity few hours before sunrise. There are inverse heat islands during the afternoon for all weather types but the major frequencies are associated with the most humid and cloudy air masses type W++ and SE.

Table 7. Hourly frequencies (%) of $\Delta T_{u-r} \geq 0$ for each air mass type

	C++	S	W+	SW	W++	SE
03:00 LT	98.1	91.4	94.0	92.6	76.6	98.7
09:00 LT	98.1	94.5	91.2	95.7	68.9	96.5
15:00 LT	69.1	75.5	56.2	86.0	47.4	63.5
21:00 LT	96.3	97.1	94.6	94.3	83.8	98.3

The hourly frequencies of occurrence of seven categories of UHI intensity, for the six winter air masses, are given in Fig. 3. UHI values were categorized by magnitude in ‘bins’ defined by increments of 1 °C between − 1 °C and 4 °C. Two additional ‘bins’ held the values that were less than − 1 °C and greater than 4 °C. The plots show that the frequency distributions of the individual air masses are quite similar during the night and early morning hours. All air masses at all times show that the negative UHI events have their highest frequencies in the interval

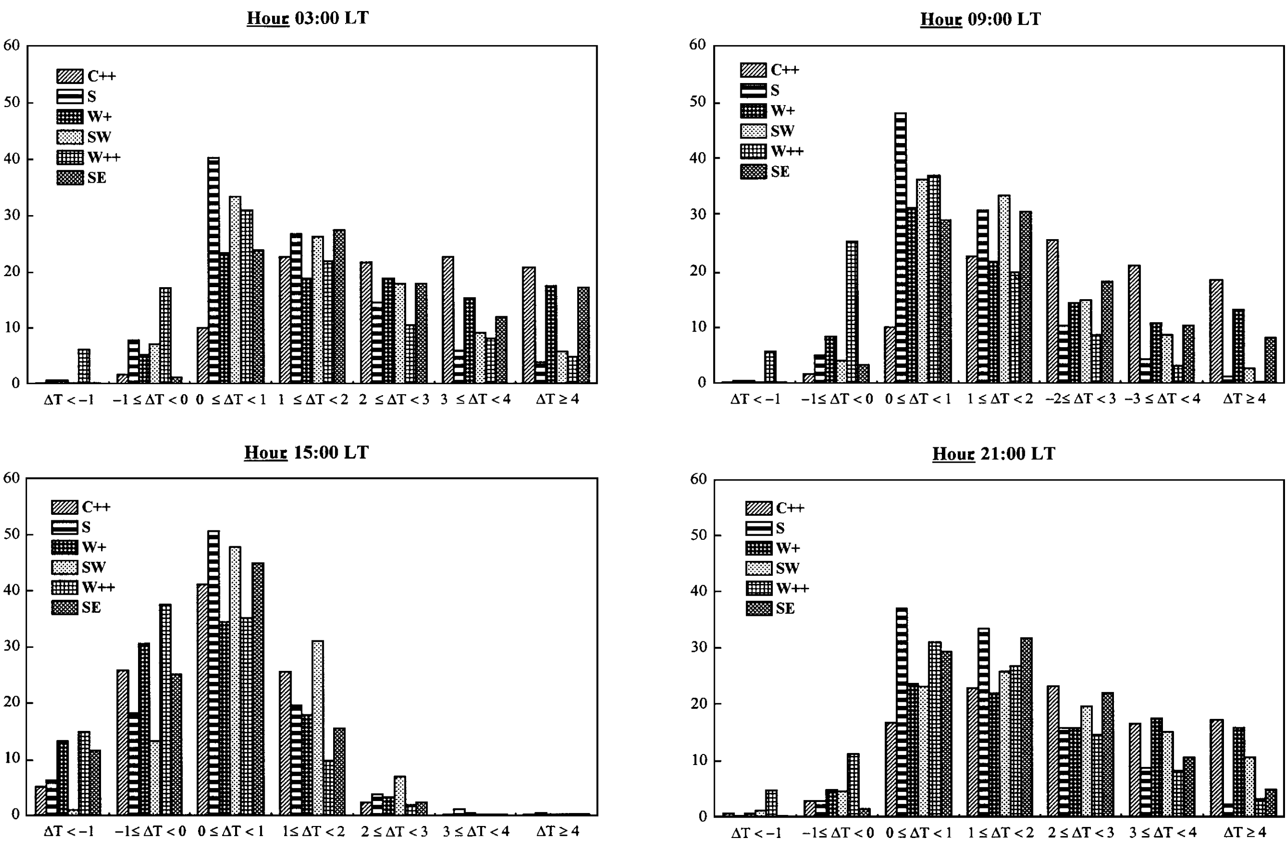

Fig. 3. Hourly frequencies (%) of occurrence of UHI intensity categories for the different air mass types

– 1 °C to 0 °C. The largest positive UHI intensities ($\Delta T_{u-r} \geq 4$ °C) at 03:00 LT and 09:00 LT are especially associated with the coldest air masses at those times (C++, W+ and SE), but at 21:00 LT the largest frequencies for that UHI intensity category are observed for air masses with minimum cloud cover (C++, W+ and SW). At 15:00 LT the frequencies for the categories of UHI magnitudes greater than 3 °C are almost null for all air masses all but air mass W++, show their maximum frequencies in the interval 0–1 °C.

5. Concluding remarks

The goal of this study was to apply a statistically objective method to classify weather types for winter days in Buenos Aires, Argentina. The weather types or air masses were defined considering the 03:00, 09:00, 15:00 and 21:00 LT surface observations of dry bulb temperature, dew point, cloud cover, atmospheric pressure and wind direction and velocity at the rural station Ezeiza. The clustering method K-means segregated six air masses that were used to analyze the Buenos Aires UHI intensity under different weather types. Results indicate that the mean UHI intensity is highest a few hours before sunrise when conditions are dominated by the coldest air mass C++ associated with cold-core anticyclones, weak winds and low cloud cover. An inverse heat island is found during the afternoon for all air masses indicating that surface processes are not dominant at that time. The relatively infrequent air mass W++ is the only one that presents a mean negative urban–rural temperature difference during the afternoon with the smallest diurnal cycle of the UHI intensity probably due to the prevailing high humidity and cloudy skies. In summary, the paper provides an insight into the Buenos Aires urban–rural temperature difference under a variety of winter weather types and could be used to improve local daily temperature forecasts for the metropolitan area of Buenos Aires on the basis of the routine forecast of weather types.

Acknowledgement

This work was done with the support of X084 University of Buenos Aires grant. The authors would like to express their appreciation to Prof. Tim Oke and two anonymous reviewers who contributed to improve this manuscript.

References

Barros VR, Camilloni IA (1994) Urban-biased trends in Buenos Aires' mean temperature. Clim Res 4: 33–45

Bornstein RD (1968) Observations of the urban heat island effect in New York City. J Appl Meteor 7: 575–582

Brook JR, Samson PJ, Sillman S (1995a) Aggregation of selected three-day periods to estimate annual and seasonal wet deposition totals for sulfate, nitrate and acidity. Part I: A synoptic and chemical climatology for eastern North America. J Appl Meteor 34: 297–325

Brook JR, Samson PJ, Sillman S (1995a) Aggregation of selected three-day periods to estimate annual and seasonal wet deposition totals for sulfate, nitrate and acidity. Part II: Selection of events, deposition totals and source-receptor relationships. J Appl Meteor 34: 326–339

Camilloni IA (1999) Temporal variability of the Buenos Aires' urban heat island intensity. Proceedings of the 15th International Congress of Biometeorology & International Conference on Urban Climatology ICB-ICUC'99 (CD-ROM). Australia

Camilloni IA, Mazzeo NA (1987) Algunas características térmicas de la atmósfera urbana de Buenos Aires. Preprints of II Congreso Interamericano de Meteorología y V Congreso Argentino de Meteorología, 14.2: 1–5

Camilloni IA, Barros VR (1997) On the urban heat island effect dependence on temperature trends. Climatic Change 37: 665–681

Colacino M, Rovelli A (1983) Yearly averaged air temperature in Rome from 1782 to 1975. Tellus A 35: 389–397

Dorling SR, Davies TD, Pierce CE (1992a) Cluster analysis: A technique for estimating the synoptic meteorological controls on air and precipitation chemistry – method and applications. Atmos Environ 26A: 2575–2581

Dorling SR, Davies TD, Pierce CE (1992b) Cluster analysis: A technique for estimating the synoptic meteorological controls on air and precipitation chemistry – results from Eskdalemuir, south Scotland. Atmos Environ 26A: 2583–2602

Figuerola PI, Mazzeo NA (1998) Urban–rural temperature differences in Buenos Aires. Int J Climatol 18: 1709–1723

Greene JS, Kalkstein LS, Ye H, Smoyer K (1999) Relationships between synoptic climatology and atmospheric pollution at 4 US cities. Theor Appl Climatol 62: 163–174

Kalkstein LS, Nichols MC, Barthel CD, Greene JS (1996) A new spatial synoptic classification: application to air-mass analysis. Int J Climatol 16: 983–1004

Kalkstein LS, Sheridan SC, Graybeal DY (1998) A determination of character and frequency changes in air masses using a spatial synoptic classification. Int J Climatol 18: 1223–1236

Kalkstein LS, Tan G, Skindlov JA (1987) An evaluation of three clustering procedures for use in synoptic climatological classification. J Climate Appl Meteor 26: 717–730

Kalnay E, Coauthors (1996) The NCEP/NCAR 40-year reanalysis project. Bull Amer Meteor Soc 77: 437–471

Karl TR, Diaz HF, Kukla G (1988) Urbanization: its detection and effect in the United States climate record. J Climate 1: 1099–1123
Kidder SQ, Essenwanger OM (1995) The effect of clouds and wind on the difference in nocturnal cooling rates between urban and rural areas. J Appl Meteor 34: 2440–2448
Lamb HH (1972) British Isles weather types and a register of the daily sequence of circulation patterns, 1861–1972 (updated to 1977). Meteorological Office Geophysical Memoirs 116: 49
Landsberg H (1981) The urban climate. New York: Academic Press, 275 pp
Lowry W (1977) Empirical estimation of urban effects on problem analysis. J Appl Meteor 16: 124–135
Mc Queen J (1967) Some methods for classification and analysis of multivariate observations. Proc. Fifth Berkley Symposium on Mathematical Statistics and Probability, Berkeley, CA, Univ. of California Press, pp 281–297
Michelangeli PA, Vantard R, Legras B (1995) Weather regimes: recurrence and quasi-stationarity. J Atmos Sci 52: 1237–1256
Moreno-García MC (1994) Intensity and form of the urban heat island in Barcelona. Int J Climatol 14: 705–710.2
Morris CJG, Simmonds I (2000) Associations between varying magnitudes of the urban heat island and the synoptic climatology in Melbourne, Australia. Int J Climatol 20: 1931–1954
Morris CJG, Simmonds I, Plummer N (2001) Quantification of the influences of wind and cloud on the nocturnal urban heat island of a large city. J Appl Meteor 40: 169–182
Oke TR (1973) City size and the urban heat island. Atmos Environ 7: 769–779
Oke TR (1979) Review of Urban Climatology. WMO Tech. Note No. 169, 100 pp
Oke TR (1982) The energetic basis of the urban heat island. Quart J Roy Meteor Soc 108: 1–24
Oke TR (1998) An algorithmic scheme to estimate hourly heat island magnitude. Preprints of the Second Urban Environment Symposium. American Meteorological Society, Albuquerque, USA, pp 80–83
Robertson AW, Ghil M (1999) Large-scale weather regimes and local climate over the western United States. J Climate 12: 1796–1813
Runnalls KE, Oke TR (2000) Dynamics and controls of the near-surface heat island of Vancouver, British Columbia. Physical Geography 21: 283–304
Sheridan SC, Kalkstein LS, Scott JM (1999) An evaluation of the variability of air mass character between urban and rural areas. Proceedings of the 15th International Congress of Biometeorology & International Conference on Urban Climatology ICB-ICUC'99 (CD-ROM). Australia
Spath H (1980) Cluster analyses algorithms for data reduction and classification of objects. Chicester: Ellis Horwood
Unger J (1996) Heat island intensity with different meteorological conditions in a medium-sized town: Szeged, Hungary. Theor Appl Climatol 54: 147–151
Unwin DJ (1980) The synoptic climatology of Birmingham's urban heat island, 1965–74. Weather 35: 43–50
Yague C, Zurita E, Martinez A, Statistical analysis of the Madrid urban heat island. Atmos Environ 25: 327–332
Yarnal B (1993) Synoptic Climatology in Environmental Analysis. London: Belhaven Press, 194 pp
Yarnal B, Comrie AC, Frakes B, Brown DP (2001) Developments and prospects in synoptic climatology. Int J Climatol 21: 1923–1950

Authors' addresses: Rubén A. Bejarán (e-mail: bejaran@at.fcen.uba.ar), Department of Atmospheric Sciences, University of Buenos Aires, Ciudad Universitaria, Pabellón 2, Piso 2, 1428 Buenos Aires, Argentina; Inés A. Camilloni (e-mail: inesc@at.fcen.uba.ar), Department of Atmospheric Sciences/Centro de Investigaciones del Mar y la Atmósfera (CIMA), University of Buenos Aires – CONICET, Ciudad Universitaria, Pabellón 2, Piso 2, 1428 Buenos Aires, Argentina.